

Precision determination of the $5d\ ^2D_{3/2}$ state lifetime of single $^{174}\text{Yb}^+$ ionH. Shao^{1,2}, H. Yue^{1,2,3}, Z. Ma^{1,2,3}, Y. Huang^{1,2}, H. Guan^{1,2,4,*} and K. Gao^{1,2,5,6,†}¹State Key Laboratory of Magnetic Resonance and Atomic and Molecular Physics, Innovation Academy of Precision Measurement Science and Technology, Chinese Academy of Sciences, Wuhan 430071, China²Key Laboratory of Atomic Frequency Standards, Innovation Academy of Precision Measurement Science and Technology, Chinese Academy of Sciences, Wuhan 430071, China³University of Chinese Academy of Sciences, Beijing 100049, China⁴Wuhan Institute of Quantum Technology, Wuhan 430206, China⁵Hefei National Research Center for Physical Sciences at the Microscale and School of Physical Sciences, University of Science and Technology of China, Hefei 230026, China⁶CAS Center for Excellence in Quantum Information and Quantum Physics, University of Science and Technology of China, Hefei 230026, China

(Received 20 February 2023; accepted 13 June 2023; published 27 June 2023)

We present a method to precisely determine the $^2D_{3/2}$ state lifetime of a single trapped $^{174}\text{Yb}^+$ ion. This method is based on the detection of photons emitted from excited states, where a highly synchronized measurement sequence for laser control and an intensity-alternating sequence for atomic excitation and photon counting are used to minimize systematic errors. This method is easy to implement and is immune to fluctuations of magnetic field, laser intensity, and frequency detuning. Combined with the real-time approach of background photon correction, the radiative lifetime of the $^2D_{3/2}$ state is determined to be 54.83 ± 0.18 ms, which represents an order of magnitude improvement in measurement precision. The accurately determined lifetime sets a benchmark for many-body atomic theories and is particularly useful to determine the coherence time limit of the optical clock.

DOI: [10.1103/PhysRevResearch.5.023193](https://doi.org/10.1103/PhysRevResearch.5.023193)

I. INTRODUCTION

The trapped ytterbium ion Yb^+ is an ideal system for a wide range of applications due to the environmental isolation and long coherence time of internal electronic states. In recent years, the Yb^+ ion has attracted much attention in quantum precision measurements. Since Yb^+ possesses several long natural lifetime states [1–3], of which the higher quality factor Q value can be used to develop an optical clock [4–7]. In addition, Yb^+ has many applications in testing existing physical laws and exploring new physics, such as the parity nonconservation effects arising from the electroweak interaction [8,9], new force from isotope shift studies [10,11], the Einstein's equivalence principle by testing local Lorentz symmetry [6,12], and local position invariance [13,14]. Furthermore, thanks to the commercial availability of required lasers, the ground-state hyperfine structure of Yb^+ can be considered as an effective tool to study quantum computing [15,16], quantum simulation [17], the quantum phase transition [18–20], the non-Hermitian Hamiltonian with parity-time-reversal symmetry [21], and quantum sensors [22], etc.

In the field of frequency metrology, ytterbium provides more than one clock transition line: the electric octupole transition (E3: $^2S_{1/2} - ^2F_{7/2}$) and the electric quadrupole transition (E2: $^2S_{1/2} - ^2D_{3/2}$ and $^2S_{1/2} - ^2D_{5/2}$), with the natural linewidth being nano-Hz and Hz level, respectively. However, the natural linewidth is essentially determined by the lifetime of associated excited state, which in turn determines the performance (theoretical limit of stability) of an optical clock. In particular, for the longer lived $^2F_{7/2}$ state, conventional measurement methods [23,24] of directly observing the spontaneous decay becomes challenging. Measured values usually have large deviations and uncertainties over long periods of time due to competing processes such as collisions with background gases, off-resonant laser radiation, and the long measurement cycles necessary to achieve sufficiently small statistical uncertainties. Recently, Lange *et al.* [1] developed a new method by simultaneously measuring the resonant Rabi frequency and the induced quadratic Stark shift, combining the result with information on the dynamic differential polarizability; they determined the $^2F_{7/2}$ state lifetime of 1.58(8) yr, an order-of-magnitude improvement over previous experimental results.

However, due to the presence of the core-excited $4f^{13}F$ state in Yb^+ ion, the D state lifetime is difficult to calculate accurately. Early theoretical prediction for the $^2D_{3/2}$ state lifetime is 74 ms by Gerz *et al.* [25]. Fawcett and Wilson [26] used a semiempirical method and determined this lifetime to be 41 ms. Using the Hartree-Fock method with the core polarizability (HFR + CP), Biémont *et al.* [27,28] calculated the $^2D_{3/2}$ state lifetime and found that its lifetime

*guanhua@apm.ac.cn

†klgao@apm.ac.cn

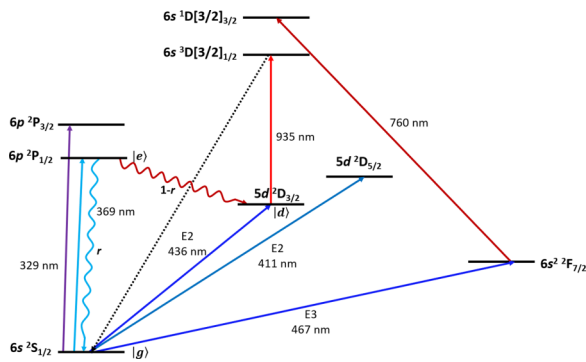


FIG. 1. Yb^+ energy-level diagram of low-lying states (not to scale).

is 51.8 ms. Recently, Nandy and Sahoo employed the relativistic coupled-cluster (RCC) method to calculate the lifetime to be 50.78 ± 50 ms [29]. From the experimental side, using the background gas collision depopulation method, Gerz *et al.* [25] measured the $^2D_{3/2}$ state lifetime to be 52.15 ± 1 ms. Later, Yu and Maleki [2] performed measurements on single $^{174}\text{Yb}^+$ ion by detecting emitted photons from $^2P_{1/2}$ to the ground state $^2S_{1/2}$, and determined the $^2D_{3/2}$ state lifetime of 52.7 ± 2.4 ms. Combined with the measured results of Yu and Maleki [2], Biémont *et al.* [30] improved their theoretical calculation and obtained the lifetime of 52.8 ms. Recently, Schacht *et al.* [31] performed the $^{171}\text{Yb}^+$ ion $^2D_{3/2}$ ($F = 2$) state lifetime measurement. After a certain waiting time, the continuous fluorescence signal was monitored by fluorescence detection with the 369-nm cooling and 935-nm pumping lasers turned on to distinguish whether the ion was still in the $^2D_{3/2}$ ($F = 2$) state or had undergone spontaneous emission from $^2D_{3/2}$ ($F = 2$) to the ground state $^2S_{1/2}$. The determined lifetime is $61.8 \pm (0.6)_{\text{stat}} \pm (6.4)_{\text{sys}}$ ms, which is a factor of 4 improvement on the statistical uncertainty but is significantly larger than other measurements. It is clear that there are significant discrepancies between theoretical and experimental values for the $^2D_{3/2}$ state lifetime.

To experimentally resolve the existing discrepancies for the $^2D_{3/2}$ state lifetime, here we adopt an experimental approach by counting the scattered photons $\langle N \rangle$ from the excited $^2P_{1/2}$ state to the $^2S_{1/2}$ ground state. This method is immune to fluctuations of laser light intensity, frequency detuning, and magnetic field, and has been used to measure $^2P_{1/2}$ branching fraction of $^{40}\text{Ca}^+$ [32] and $^2D_{3/2}$ lifetime of $^{174}\text{Yb}^+$ [2]. Compared with [2], background photon subtraction in a real-time way and intensity-alternating sequence for reducing detection error are used here. The energy-level diagram of $^{174}\text{Yb}^+$ is shown in Fig. 1.

II. EXPERIMENTAL PROCEDURE

The single ion was loaded in a miniature four-blade linear Paul trap by using the ablation technique [33] combined with ionization lasers, 399 and 369 nm. The details of this trap can be found in Ref. [34]. Excessive micromotion of ion was well compensated by monitoring position changes in a charge-coupled device (CCD) and by using the rf photon correlation method. The ion trap was installed in an ultrahigh vacuum chamber with a background pressure less than 1.0×10^{-8} Pa

to reduce the deexcitation caused by the collision between the ions and background gases and ensure a stable measurement environment.

The Yb^+ ion was Doppler cooled primarily using the $^2S_{1/2} - ^2P_{1/2}$ dipole transition at 369 nm because of the short lifetime of the excited state [35]. The light power and waist were $20 \mu\text{W}$ and $38 \mu\text{m}$, respectively. Due to the decay from $^2P_{1/2}$ to $^2D_{3/2}$ [36], the re-pumping laser light at 935 nm with a power of $320 \mu\text{W}$ and a waist of $135 \mu\text{m}$ enabled a fast depletion of the excited clock state via the $^3D[3/2]_{1/2}$ state back to the ground state, thereby keeping the photon counting rate at an acceptably high level. In order to achieve a multi-period continuous measurement, the frequency of the 935-nm pump laser was stabilized to the wavelength meter (HighFinesse WS-7). The 369-nm light with a power of $135 \mu\text{W}$ and a beam waist of $46 \mu\text{m}$ was used as a pulse of alternating intensity to excite the emitted photons, with its frequency being locked to a standard Fabry-Pérot cavity ($\mathcal{F} = 7500$), which is made of ultralow expansion (ULE) according to the Pound-Drever-Hall scheme, making the linewidth about 200 kHz. The signal detection was realized by the 369-nm fluorescence generated by the spontaneous decay of the ion from $^2P_{1/2}$ to $^2S_{1/2}$ and was monitored by a Hamamatsu photomultiplier tube (PMT). The scattered background light was filtered from the fluorescence signal by two narrow-bandpass filters and a pinhole with diameter of $40 \mu\text{m}$. A computer was used to record all experimental data and control the photon-counter, all acousto-optic modulators (AOMs), and mechanical shutters simultaneously via a field programmable gate array (FPGA) at the accuracy of nanosecond level. To avoid low-frequency magnetic field noise, the vacuum chamber was surrounded by two layers of μ -metal shielding, and a low-noise current source was used. A large magnetic field about $800 \mu\text{T}$ and linear polarization of the laser lights were used to avoid any optical pumping and coherent population trapping. All laser beams were guided through its corresponding wavelength single-mode polarization-maintaining (PM) fibers to the ions, and a polarization matching was employed by using quarter and half waveplates in front of the fiber couplers.

To prepare the initial $^2D_{3/2}$ state for spontaneous decay, the 369-nm laser was applied to incoherently shelve the ion into that state when the 935-nm light was absent. It is noted that the state $^2D_{3/2}$ is connected to the cooling transition and photon detection. Any attempt to detect fluorescence by switching on the two lasers at 369 and 935 nm destroys the state of the free decaying ions. Therefore it is necessary to let the ion remain undisturbed for a period of time in the $^2D_{3/2}$ state and determine whether the spontaneous decay occurs by detecting the photon count emitted from the $^2P_{1/2} - ^2S_{1/2}$ transition at 369 nm.

A simplified sequence and associated energy-level diagram describing the lifetime measurement of the $^2D_{3/2}$ state are depicted in Fig. 2. The sequence consists of five major steps for one round of measurement. In the first step, a frequency-red-detuned 369-nm (-15 MHz) laser and a frequency-resonant 935-nm laser with the ion were employed for 10 ms for the cooling cycle, and the ions were laser-cooled to the Lamb-Dicke regime. Afterwards, an additional 1-ms 935-nm quenching laser was applied to excite the ion from $^2D_{3/2}$ to

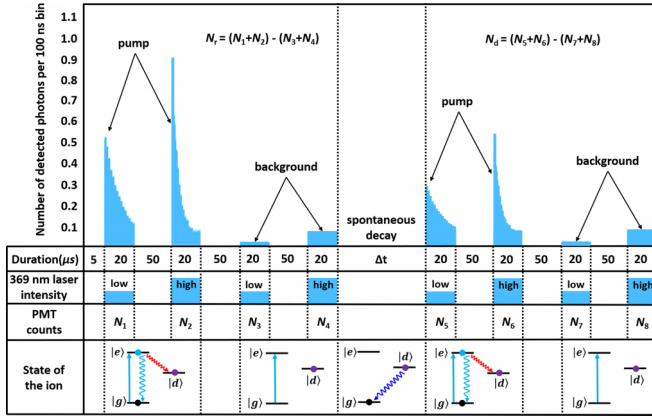


FIG. 2. Simplified sequence and associated energy-level diagram (not to scale) depicting lifetime measurements for single Yb^+ ion in the $^2D_{3/2}$ state.

$^3D[3/2]_{1/2}$, ensuring that the ion was indeed in the ground state. In the second step, two $20\ \mu\text{s}$, 369 nm, and frequency nearly resonant laser pulses, where one pulse’s power was saturated and the other one half the saturated, were used to excite a $^2S_{1/2} - ^2P_{1/2}$ transition, inducing an incoherent shelving to the $^2D_{3/2}$ state, denoted as N_1 and N_2 . These two pulses were then used to background subtraction ($N_3 + N_4$). In this population the number of detected photons scattered from $^2P_{1/2}$ to $^2S_{1/2}$ was $N_r = (N_1 + N_2) - (N_3 + N_4)$. In the third step a waiting time Δt was implemented and all lasers were turned off while the AOM and the mechanical shutter were synchronized to avoid residual light restimulating the relevant transitions, maintaining spontaneous decay with no light disturbing this process. In the fourth step, to verify whether the ion had decayed from the $^2D_{3/2}$ to the ground state, we applied another set of two $20\text{-}\mu\text{s}$, 369-nm laser pulses, where one pulse’s power was saturated and the other half the saturated one, with the photon counting numbers being N_5 and N_6 , respectively. Then we applied another set of the same pulses to do the background subtraction ($N_7 + N_8$). In order to minimize the counting rate error and other errors associated with the PMT dead time, each pulse was assigned a different intensity. If the ion was decayed to the $^2S_{1/2}$ state, it could be pumped to the $^2P_{1/2}$ state, and the photon count for the emission from $^2P_{1/2}$ to $^2S_{1/2}$ by the 369-nm light could be detected as $N_d = (N_5 + N_6) - (N_7 + N_8)$. If not, the fluorescence remained at the background level. Therefore the spontaneous decay probability P of the ions from $^2D_{3/2}$ to the ground state $^2S_{1/2}$ with wait time Δt can be defined by $P = N_d/N_r$. In the last step, the cooling and repumping lasers were switched on for 5 ms and the PMT count, denoted as N_9 , discriminated whether the ions were kept in the cooling cycle (“bright”), or in the $^2F_{7/2}$ state (“dark”) by collision with background gases. A valid interrogation cycle ended with reappearance of the fluorescence signal until the next cooling period. Here a high-precision and highly synchronized measurement sequence were used with the alternating intensity for atomic excitation and photon counting to minimize counting rate error due to the PMT dead time. A real-time detection method was implemented to minimize background photon counting errors caused by laser intensity fluctuations.

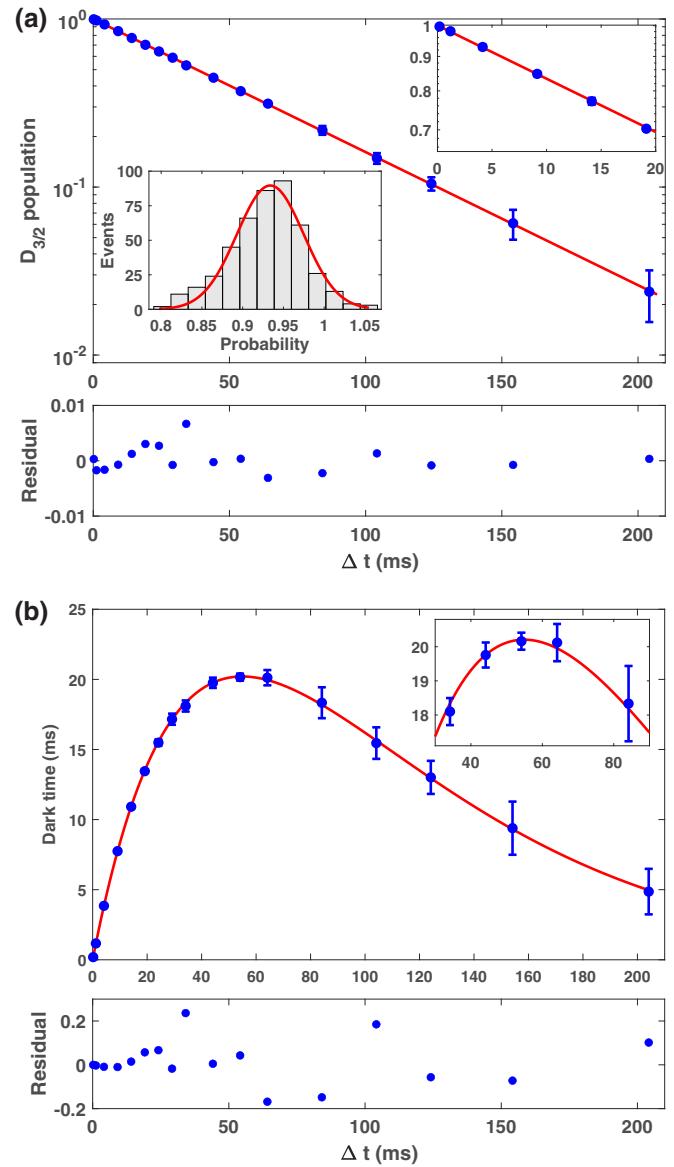


FIG. 3. Two fittings to the data points for the $^2D_{3/2}$ state lifetime measurement in $^{174}\text{Yb}^+$. (a) The fitting curve determined by the method of linear regression and least-squares fit. The lower-left inset shows the verified results of the normal distribution. (b) The fitting curve determined by the maximum likelihood fit, where the lower diagram shows the residuals between the data points and the fitting curve.

III. RESULTS AND DISCUSSION

In our experiment, measurements were repeated over 600 000 times for each wait time Δt , with Δt set from 0.05 to 204 ms. The $^2D_{3/2}$ state lifetime was then determined from the exponential law $1 - P = \exp(-\Delta t/\tau_{3/2})$. Using the measured data points shown in Fig. 3(a), we obtained the natural lifetime $\tau_{3/2} = 54.82 \pm 0.17$ ms by linear regression and least-squares fitting. Furthermore, the mean time for an ion to be detected in the $^2D_{3/2}$ state during Δt was determined by $\Delta t(1 - P) = \Delta t \exp(-\Delta t/\tau_{3/2})$. Using the measured data points shown in Fig. 3(b) and the maximum likelihood method yielded the lifetime $\tau_{3/2} = 54.83 \pm 0.09$ ms. The confidence

interval is 2σ standard uncertainty in these two estimations of $\tau_{3/2}$. Here we take the mean of these two independent determinations and the larger uncertainty as our final lifetime $\tau_{3/2} = 54.83 \pm 0.17$ ms. For each probability at different Δt , we carried out a large number of measurements to reduce statistical uncertainty. Since the spontaneous decay probability follows a normal distribution, the statistical uncertainty can be effectively reduced by averaging. The normal distribution can be verified by measuring the spontaneous decay probability from ${}^2D_{3/2}$ to ${}^2S_{1/2}$ at any wait time Δt . Here we take $\Delta t = 9$ ms as an example, as shown in the lower-left inset of Fig. 3(a). Each event represents 2000 experimental cycles, and 450 such events (total of 450×2000 measurement cycles) occurred to study the probability distribution, which shows the normal distribution $f(p) = \frac{1}{\sqrt{2\pi}\sigma} \exp(-\frac{(p-\mu)^2}{2\sigma^2})$, where the mean number is $\mu = 0.9339$, and the variance is $\sigma = 0.041$. We also checked the results using statistical tools such as the χ^2 -square test and found that the results indeed represent a normal distribution with $\chi^2 = 0.9905$.

To discriminate, the shelved ${}^2D_{3/2}$ state ion still stays in there or has been decayed to the ground state ${}^2S_{1/2}$ after wait time Δt by indirectly detecting emitted photons $\langle N \rangle$ from ${}^2P_{1/2}$ to ${}^2S_{1/2}$. We adopted this measuring scheme, the $\langle N \rangle$ is insensitive to the light intensity, frequency detuning, and is already known to be insensitive to the magnetic field strength and direction [32], which we have demonstrated experimentally. However, collision with background gases, imperfect optical pumping, and state detection are still some factors affect the measured lifetime $\tau_{3/2}$.

One of the main factors was collisions between individual ions with the background gases. When the background pressure was less than 1.0×10^{-8} Pa, an average of 0.88(34) quantum jumps was observed per hour in different periods (data accumulated over 230 h and the measurement time lasted over three months), resulting in a maximum collision rate of $2.45(94) \times 10^{-4} \text{ s}^{-1}$, which contributes to the ${}^2D_{3/2}$ state lifetime $\delta\tau_{3/2} = 0.0008(3)$ ms.

Laser-imperfect shelving will induce a different $\langle N \rangle$ compared with resonance. Imperfect shelving caused by 369 nm was matched by increasing the laser power until the shelving probability to ${}^2D_{3/2}$ reached 1. Thus the background fluorescence counts ($N_3 + N_4$) were equal to the fluorescence counts in the absence of ion within the same detection pulses. With power-saturated setting ($\geq 50 \mu\text{W}$), nearly no ($N_3 + N_4$) was observed larger than background value under statistical uncertainty in our experimental data. The data ($N_3 + N_4$) larger than background were also checked and removed during data processing afterwards. Imperfect shelving caused by 935 nm was eliminated by setting the laser power to a saturated level and frequency resonant with the ${}^2D_{3/2} - {}^3D[3/2]_{1/2}$ transition. With these operations, laser-imperfect shelving has no effect on the measured lifetime.

The state detection error was another factor. The error caused by the Poissonian noise is at the level of 10^{-6} [37], which can be neglected. The errors caused by the spontaneous decay during the detection periods of N_r and N_d have the same decay rate in the same time interval, so they cancel each other out, leaving the measured lifetime unaffected.

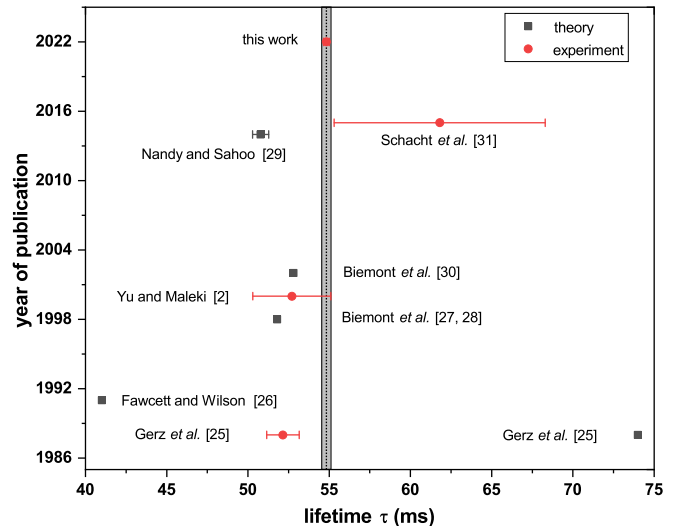


FIG. 4. Comparison of experimental (red) and theoretical (gray) ${}^2D_{3/2}$ state lifetime.

After the above statistical and systematic analysis, we arrive at the final result of the ${}^{174}\text{Yb}^+ {}^2D_{3/2}$ state lifetime, $\tau_{3/2} = 54.83 \pm 0.18$ ms. A comparison of experimental (red) and theoretical (gray) values of the ${}^2D_{3/2}$ lifetime is shown in Fig. 4. One can see that our result is in marginal agreement with the measured value of Yu and Maleki [2] but with a 13-fold improvement in precision.

IV. CONCLUSIONS

In summary, we adopted a measurement method to detect spontaneous emission of photons from an excited atom and investigated the ${}^{174}\text{Yb}^+ {}^2D_{3/2}$ state lifetime, because the ${}^{174}\text{Yb}^+$ ion provides easier measurement due to higher fluorescence [38]. We greatly reduced the measurement uncertainties, and our result rather serves as the most precise measurement to date. One of the advantages of this method is that it is not affected by fluctuations in excitation light intensity and frequency. Also, any Doppler shift due to temperature and the ion micromotion will not affect the photon number $\langle N \rangle$. Furthermore, the state with $J = 1/2$ provides additional insensitivity to the magnitude and direction of the magnetic field. Here we employed a high-precision and highly synchronized laser-controlled measurement sequence and pulses of alternating intensity for atomic excitation and photon counting to minimize the counting rate error due to the PMT dead time. A real-time detection method was implemented to minimize background photon counting errors caused by laser intensity fluctuations. Our method can be universally applied to lifetime and branching fraction measurements of other ions and atoms with a similar structure.

ACKNOWLEDGMENTS

We thank Z.-C Yan and M. S. Safronova for fruitful discussions. This work is supported by the National Basic Research Program of China (Grant No. 2021YFF0603801), the National Natural Science Foundation of China (Grants

No. 12204491 and No. 12121004), the Wuhan Young Talent Program (Grant No. R22H000106), the CAS Youth Innovation Promotion Association (Grants No. 2018364 and No. Y201963), the CAS Project for Young Scientists in Basic

Research (Grant No. YSBR-055), the Natural Science Foundation of Hubei Province (Grant No. 2022CFA013), the Chinese Academy of Sciences, and Wuhan Institute of Quantum Technology.

-
- [1] R. Lange, A. A. Peshkov, N. Huntemann, C. Tamm, A. Surzhykov, and E. Peik, Lifetime of the $^2F_{7/2}$ Level in Yb^+ for Spontaneous Emission of Electric Octupole Radiation, *Phys. Rev. Lett.* **127**, 213001 (2021).
- [2] N. Yu and L. Maleki, Lifetime measurements of the $4f^{14}5d$ metastable states in single ytterbium ions, *Phys. Rev. A* **61**, 022507 (2000).
- [3] T. R. Tan, C. L. Edmunds, A. R. Milne, M. J. Biercuk, and C. Hempel, Precision characterization of the $^2D_{5/2}$ state and the quadratic Zeeman coefficient in $^{171}\text{Yb}^+$, *Phys. Rev. A* **104**, L010802 (2021).
- [4] R. M. Godun, P. B. R. Nisbet-Jones, J. M. Jones, S. A. King, L. A. M. Johnson, H. S. Margolis, K. Szymaniec, S. N. Lea, K. Bongs, and P. Gill, Frequency Ratio of Two Optical Clock Transitions in $^{171}\text{Yb}^+$ and Constraints on the Time Variation of Fundamental Constants, *Phys. Rev. Lett.* **113**, 210801 (2014).
- [5] N. Huntemann, C. Sanner, B. Lipphardt, Chr. Tamm, and E. Peik, Single-Ion Atomic Clock with 3×10^{-18} Systematic Uncertainty, *Phys. Rev. Lett.* **116**, 063001 (2016).
- [6] C. Sanner, N. Huntemann, R. Lange, Ch. Tamm, E. Peik, M. S. Safronova and S. G. Porsev, Optical clock comparison for Lorentz symmetry testing, *Nature (London)* **567**, 204 (2019).
- [7] W. Zhuang, T.-G. Zhang, and J.-B. Chen, An active ion optical clock, *Chin. Phys. Lett.* **31**, 093201 (2014).
- [8] S. G. Porsev, M. S. Safronova, and M. G. Kozlov, Correlation effects in Yb^+ and implications for parity violation, *Phys. Rev. A* **86**, 022504 (2012).
- [9] B. K. Sahoo and B. P. Das, Parity nonconservation in ytterbium ion, *Phys. Rev. A* **84**, 010502(R) (2011).
- [10] I. Counts, J. Hur, D. P. L. Aude Craik, H. Jeon, C. Leung, J. C. Berengut, A. Geddes, A. Kawasaki, W. Jhe, and V. Vuletić, Evidence for Nonlinear Isotope Shift in Yb^+ Search for New Boson, *Phys. Rev. Lett.* **125**, 123002 (2020).
- [11] J. Hur, D. P. L. Aude Craik, I. Counts, E. Knyazev, L. Caldwell, C. Leung, S. Pandey, J. C. Berengut, A. Geddes, W. Nazarewicz, P. Reinhard, A. Kawasaki, H. Jeon, W. Jhe, and V. Vuletić, Evidence of Two-Source King Plot Nonlinearity in Spectroscopic Search for New Boson, *Phys. Rev. Lett.* **128**, 163201 (2022).
- [12] L. S. Dreissen, C.-H. Yeh, H. A. Furst, K. C. Grensemann, and T. E. Mehlstäubler, Improved bounds on Lorentz violation from composite pulse Ramsey spectroscopy in a trapped ion, *Nat. Commun.* **13**, 7314 (2022).
- [13] R. Lange, N. Huntemann, J. M. Rahm, C. Sanner, H. Shao, B. Lipphardt, C. Tamm, S. Weyers, and E. Peik, Improved Limits for Violations of Local Position Invariance from Atomic Clock Comparisons, *Phys. Rev. Lett.* **126**, 011102 (2021).
- [14] N. Huntemann, B. Lipphardt, C. Tamm, V. Gerginov, S. Weyers, and E. Peik, Improved Limit on a Temporal Variation of m_p/m_e from Comparisons of Yb^+ and Cs Atomic Clocks, *Phys. Rev. Lett.* **113**, 210802 (2014).
- [15] K. Wright, K. M. Beck, S. Debnath, J. M. Amini, Y. Nam, N. Grzesiak, J.-S. Chen, N. C. Pisenti, M. Chmielewski, C. Collins, K. M. Hudek, J. Mizrahi, J. D. Wong-Campos, S. Allen, J. Apisdorf, P. Solomon, M. Williams, A. M. Ducore, A. Blinov, S. M. Kreikemeier *et al.*, Benchmarking an 11-qubit quantum computer, *Nat. Commun.* **10**, 5464 (2019).
- [16] S. Debnath, N. M. Linke, C. Figgatt, K. A. Landsman, K. Wright, and C. Monroe, Demonstration of a small programmable quantum computer with atomic qubits, *Nature (London)* **536**, 63 (2016).
- [17] C. Monroe, W. C. Campbell, L.-M. Duan, Z.-X. Gong, A. V. Gorshkov, P. W. Hess, R. Islam, K. Kim, N. M. Linke, G. Pagano, P. Richerme, C. Senko, and N. Y. Yao, Programmable quantum simulations of spin systems with trapped ions, *Rev. Mod. Phys.* **93**, 025001 (2021).
- [18] J. Zhang, G. Pagano, P. W. Hess, A. Kyprianidis, P. Becker, H. Kaplan, A. V. Gorshkov, Z.-X. Gong, and C. Monroe, Observation of a many-body dynamical phase transition with a 53-qubit quantum simulator, *Nature (London)* **551**, 601 (2017).
- [19] M.-L. Cai, Z.-D. Liu, W.-D. Zhao, Y.-K. Wu, Q.-X. Mei, Y. Jiang, L. He, X. Zhang, Z.-C. Zhou, and L.-M. Duan, Observation of a quantum phase transition in the quantum Rabi model with a single trapped ion, *Nat. Commun.* **12**, 1126 (2021).
- [20] D. Lv, S. An, Z. Liu, J. Zhang, J. S. Pedernales, L. Lamata, E. Solano, and K. Kim, Quantum Simulation of the Quantum Rabi Model in a Trapped Ion, *Phys. Rev. X* **8**, 021027 (2018).
- [21] L. Ding, K. Shi, Q. Zhang, D. Shen, X. Zhang, and W. Zhang, Experimental Determination of \mathcal{PT} -Symmetric Exceptional Points in a Single Trapped Ion, *Phys. Rev. Lett.* **126**, 083604 (2021).
- [22] I. Baumgart, J.-M. Cai, A. Retzker, M. B. Plenio, and Ch. Wunderlich, Ultrasensitive Magnetometer using a Single Atom, *Phys. Rev. Lett.* **116**, 240801 (2016).
- [23] H. Shao, Y. Huang, H. Guan, Y. Qian, and K. Gao, Precision measurement of the $3d^2D_{3/2}$ -state lifetime in a single trapped $^{40}\text{Ca}^+$, *Phys. Rev. A* **94**, 042507 (2016).
- [24] H. Shao, Y. Huang, H. Guan, C. Li, T. Shi, and K. Gao, Precise determination of the quadrupole transition matrix element of $^{40}\text{Ca}^+$ via branching-fraction and lifetime measurements, *Phys. Rev. A* **95**, 053415 (2017).
- [25] Ch. Gerz, J. Roths, F. Vedel, and G. Werth, Lifetime and collisional depopulation of the metastable $5D_{3/2}$ state of Yb^+ , *Z. Phys. D* **8**, 235 (1988).
- [26] B. C. Fawcett and M. Wilson, Computed oscillator strengths, Landé g values, and lifetimes in Yb II, *At. Data Nucl. Data Tables* **47**, 241 (1991).
- [27] E. Biémont and P. Quinet, Theoretical Study of the $4f^{14}6s^2S_{1/2} - 4f^{13}6s^2F_{7/2}^0$ E3 Transition in Yb II, *Phys. Rev. Lett.* **81**, 3345 (1998).
- [28] E. Biémont, J.-F. Dutrieu, I. Martin, and P. Quinet, Lifetime calculations in Yb II, *J. Phys. B: At. Mol. Opt. Phys.* **31**, 3321 (1998).

- [29] D. K. Nandy and B. K. Sahoo, Quadrupole shifts for the $^{171}\text{Yb}^+$ ion clocks: Experiments versus theories, *Phys. Rev. A* **90**, 050503(R) (2014).
- [30] E. Biémont, P. Quinet, Z. Dai, J. Zhankui, Z. Zhiguo, H. Xu, and S. Svanberg, Lifetime measurements and calculations in singly ionized ytterbium, *J. Phys. B: At. Mol. Opt. Phys.* **35**, 4743 (2002).
- [31] M. Schacht, J. R. Danielson, S. Rahaman, J. R. Torgerson, J. Zhang, and M. M. Schauer, $^{171}\text{Yb}^+$ $5D_{3/2}$ hyperfine state detection and $F = 2$ lifetime, *J. Phys. B: At. Mol. Opt. Phys.* **48**, 065003 (2015).
- [32] M. Ramm, T. Pruttivarasin, M. Kokish, I. Talukdar, and H. Häffner, Precision Measurement Method for Branching Fractions of Excited $P_{1/2}$ States Applied to $^{40}\text{Ca}^+$, *Phys. Rev. Lett.* **111**, 023004 (2013).
- [33] H. Shao, M. Wang, M. Zeng, H. Guan, and K. Gao, Laser ablation and two-step photo-ionization for the generation of $^{40}\text{Ca}^+$, *J. Phys. Commun.* **2**, 095019 (2018).
- [34] S. M. Brewer, J.-S. Chen, A. M. Hankin, E. R. Clements, C. W. Chou, D. J. Wineland, D. B. Hume, and D. R. Leibbrandt, $^{27}\text{Al}^+$ Quantum-Logic Clock with a Systematic Uncertainty below 10^{-18} , *Phys. Rev. Lett.* **123**, 033201 (2019).
- [35] S. Olmschenk, D. Hayes, D. N. Matsukevich, P. Maunz, D. L. Moehring, K. C. Younge, and C. Monroe, Measurement of the lifetime of the $6p^2P_{1/2}^0$ level of Yb^+ , *Phys. Rev. A* **80**, 022502 (2009).
- [36] S. Olmschenk, K. C. Younge, D. L. Moehring, D. N. Matsukevich, P. Maunz, and C. Monroe, Manipulation and detection of a trapped Yb^+ , *Phys. Rev. A* **76**, 052314 (2007).
- [37] A. Kreuter, C. Becher, G. P. T. Lancaster, A. B. Mundt, C. Russo, H. Häffner, C. Roos, W. Hänsel, F. Schmidt-Kaler, R. Blatt, and M. S. Safronova, Experimental and theoretical study of the $3d^2D$ -level lifetimes of $^{40}\text{Ca}^+$, *Phys. Rev. A* **71**, 032504 (2005).
- [38] S. Ejtemaee, R. Thomas, and P. C. Haljan, Optimization of Yb^+ fluorescence and hyperfine-qubit detection, *Phys. Rev. A* **82**, 063419 (2010).